Heliyon 9 (2023) e15584

Contents lists available at ScienceDirect

Heliyon

journal homepage: www.cell.com/heliyon

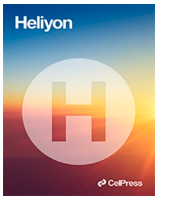

Research article

SENP3 deletion promotes M2 macrophage polarization and accelerates wound healing through smad6/IκB/p65 signaling pathway

Yiwen Ma [a,1], Jiateng Hu [b,c,1], Xingjuan Xue [d], Jianmin Gu [e], Yuyan Pan [f,**,2], Jun Yang [a,*,2]

[a] Department of Plastic and Reconstructive Surgery, Shanghai Ninth People's Hospital, Shanghai Jiao Tong University School of Medicine, Shanghai, 200011, China
[b] Department of Vascular Surgery, Shanghai Ninth People's Hospital, Shanghai Jiao Tong University School of Medicine, Shanghai, 200011, China
[c] Vascular Centre of Shanghai Jiao Tong University, Shanghai, 200011, China
[d] Department of Thoracic Surgery, Fuqing City Hospital Affiliated to Fujian Medical University, Fuqing City, Fujian Province, 350399, China
[e] Department of Thoracic Surgery, Zhongshan Hospital, Fudan University, Shanghai, 200032, China
[f] Department of Plastic and Reconstructive Surgery, Zhongshan Hospital, Fudan University, Shanghai, 200032, China

ARTICLE INFO

Keywords:
SENP3
Macrophage polarization
Inflammatory response
Wound healing
Smad6/IκB/p65 signaling pathway

ABSTRACT

Macrophages preferentially polarize to the anti-inflammatory M2 subtype in response to alterations in the wound microenvironment. SUMO-specific protease 3 (SENP3), a SUMO-specific protease, has been proven to regulate inflammation in macrophages by deSUMOylating substrate proteins, but its contribution to wound healing is poorly defined. Here, we report that SENP3 deletion promotes M2 macrophage polarization and accelerates wound healing in macrophage-specific SENP3 knockout mice. Notably, it affects wound healing through the suppression of inflammation and promotion of angiogenesis and collagen remodeling. Mechanistically, we identified that SENP3 knockout facilitates M2 polarization through the Smad6/IκB/p65 signaling pathway. SENP3 knockout elevated the expression of Smad6 and IκB. Moreover, Smad6 silencing enhanced the expression of p-p65 and proinflammatory cytokines while inhibiting the level of IκB. Our study revealed the essential role of SENP3 in M2 polarization and wound healing, which offers a theoretical basis for further research and a therapeutic strategy for wound healing.

1. Introduction

With the development of an aging society, trauma and metabolic diseases have gradually increased, and various complex wounds

* Corresponding author. Department of Plastic and Reconstructive Surgery, Shanghai Ninth People's Hospital, Shanghai Jiao Tong University School of Medicine, 639 Zhizaoju Rd, Shanghai 200011, China.
** Corresponding author. Department of Plastic and Reconstructive Surgery, Zhongshan Hospital, Fudan University, 180 Fenglin Rd, Shanghai 200032, China.
E-mail addresses: pan.yuyan@zs-hospital.sh.cn (Y. Pan), yangj1580@sh9hospital.org.cn (J. Yang).
[1] Yiwen Ma and Jiateng Hu contribute equally and should be co-first author.
[2] Jun Yang and Yuyan Pan contribute equally and should be co-corresponding author

https://doi.org/10.1016/j.heliyon.2023.e15584
Received 14 September 2022; Received in revised form 2 April 2023; Accepted 14 April 2023
Available online 25 April 2023

are becoming a severe threat to public health and placing heavy economic and psychological burdens on patients [1]. The key to wound repair is to explore the mechanism of wound healing, shorten the wound healing time and reduce scar formation. In addition to traditional skin/flap transplantation, new methods, such as tissue-engineered skin, growth factors, and stem cell therapy, have also been applied to the treatment of wounds [2,3]. However, due to the high cost of treatment, harsh material storage conditions and other defects, as well as the increasing needs of patients, it is of great significance to develop new treatment methods for wound healing (see Table 1 and 2).

Within wounds, the critical role of macrophages in regulating the inflammatory response and wound repair has been affirmed [4]. During normal wound healing, macrophages undergo a phenotypic switch from M1 to M2 [5]. Early monocytes differentiate into M1 macrophages and secrete a large number of cytotoxic mediators and proinflammatory factors, including Interleukin-1 beta (IL-1β), tumor necrosis factor (TNF-α), and interleukin-6 (IL-6), and produce nitric oxide by decomposing L-arginine, which exerts a cytotoxic effect [6]. M2 macrophages in the subsequent proliferative phase play an important role in promoting fibrosis and tissue remodeling. The secreted transforming growth factor beta (TGF-β), interleukin-10 (IL-10), vascular endothelial growth factor (VEGF) and other cytokines alleviate the inflammatory response and promote the differentiation of fibroblasts into myofibroblasts, angiogenesis, and the formation of extracellular matrix [7]. During the remodeling phase, M2 inhibits the production of L-proline and the synthesis of collagen, promotes the dissolution and absorption of extracellular matrix, and secretes IL-10 to inhibit excessive fibrosis and reduce scarring. The timely transformation of M1 macrophages into M2 macrophages promotes the progression of wound healing from the inflammatory phase to the proliferative phase [8]. Hence, modulation of macrophage polarization is a key strategy for wound healing.

Small ubiquitin-related modifier (SUMO) is an important ubiquitin-like protein. SUMOylation affects the stability, subcellular localization and transcription of proteins, thus regulating diverse biological events [9]. SUMOylation is a dynamic and reversible process in which SUMO can be removed from its substrates by the sentrin-specific protease (SENP) family [10]. SENP3 is a redox-sensitive SUMO2/3-specific protease in the SENP family that accumulates under cellular redox stress [11,12]. Reactive oxygen species (ROS) can lead to rapid increases in the nuclear level of SENP3 by inhibiting its proteasomal degradation [11,12]. SENP3 has been shown to potentiate lipopolysaccharide (LPS)-induced inflammatory signaling in macrophages via deSUMOylation of mitogen-activated protein kinase 7 (MKK7) [13]. Another study verified that SENP3 mediates LPS-induced coagulation activation by upregulating monocyte/macrophage tissue factor expression in a JNK-dependent manner [14]. The studies above indicate that SENP3 regulates the inflammatory signaling pathway in the macrophage cytoplasm by deSUMOylating substrate proteins. Thus, we presumed that SENP3 might play a role in the macrophage-mediated inflammatory response during wound healing.

To test this hypothesis, we constructed SENP3 flox/flox$^{(fl/fl)}$ Lyz2-cre mice (mice with SENP3 conditional knockout in macrophages, named SENP3 cKO mice) to explore the effect of SENP3 on macrophage polarization and the inflammatory response in wound healing. Our study confirmed that SENP3 deficiency contributes to the acceleration of wound healing by regulating macrophage polarization and the inflammatory response both *in vitro* and *in vivo*. These findings may provide a theoretical basis for further research and application in wound healing.

2. Results

2.1. SENP3 is significantly increased in macrophages during wound healing

To investigate the potential roles of SENP3 in wound healing, we first determined whether SENP3 expression was altered in wound healing. As shown in Fig. 1A and B, the expression of SENP3 in wound tissues extracted on Day 6 was significantly elevated compared with that of normal skin tissues (sham group) ($n = 6$, $P < 0.001$). Both the mRNA and protein levels of SENP3 were increased in wound tissues compared with the sham group ($n = 6$, $P < 0.001$, $P < 0.01$) (Fig. 1C–E). *In vitro*, both the mRNA and protein levels of SENP3 were increased in macrophages exposed to LPSs compared with the control group ($P < 0.01$, $P < 0.001$) (Fig. 1F–H).

2.2. SENP3 deficiency decreases inflammatory cytokine production in macrophages

We first constructed SENP3 cKO mice as shown in Fig. 2A and B. Immunofluorescence analysis indicated that SENP3 decreased in SENP3 cKO mice compared with SENP3$^{fl/fl}$ mice during wound healing ($P < 0.001$) (Fig. 2C and D). The SENP3 expression levels in the BMDMs of these mice were verified ($P < 0.001$) (Fig. 2E and F). We then determined the correlations between SENP3 levels and

Table 1
Antibodies used in Western blot.

Antibodies	Cat. No. & Company	Dilution ratio
SENP3	DF8198, Affinity	1:2000
Smad6	AF5160, Affinity	1:1000
IκB	AF5002, Affinity	1:1000
p-p65	AF2006, Affinity	1:1000
P65	AF5006, Affinity	1:1000
GAPDH	AF7021, Affinity	1:1000
β-actin	BM0627, Boster	1:500

Note: SENP3, SUMO-specific protease 3; IκB, Inhibitor of kappa B; GAPDH, glyceraldehyde-3-phosphate dehydrogenase.

Table 2
Primer nucleotide sequences of RT-qPCR.

Name	Primer sequence
m-SENP3-F	AGACTATACAGGGGACCGGG
m-SENP3-R	CGTCTAGTTGGCACTGTGGT
m-Smad6-F	TCTACGACCTACCTCAGGGC
m-Smad6-R	TTGACGAAGATGGGGTGCTC
m-IκB-F	CTCCCCCTACCAGCTTACCT
m-IκB-R	TAGGGCAGCTCATCCTCTGT
m-GAPDH-F	TGGCCTTCCGTGTTCCTAC
m-GAPDH-R	GAGTTGCTGTTGAAGTCGCA

Note: RT-qPCR, reverse transcription-quantitative polymerase chain reaction; F, forward; R, reverse; SENP3, SUMO-specific protease 3; IκB, Inhibitor of kappa B; GAPDH, glyceraldehyde-3-phosphate dehydrogenase; GAPDH, glyceraldehyde-3-phosphate dehydrogenase.

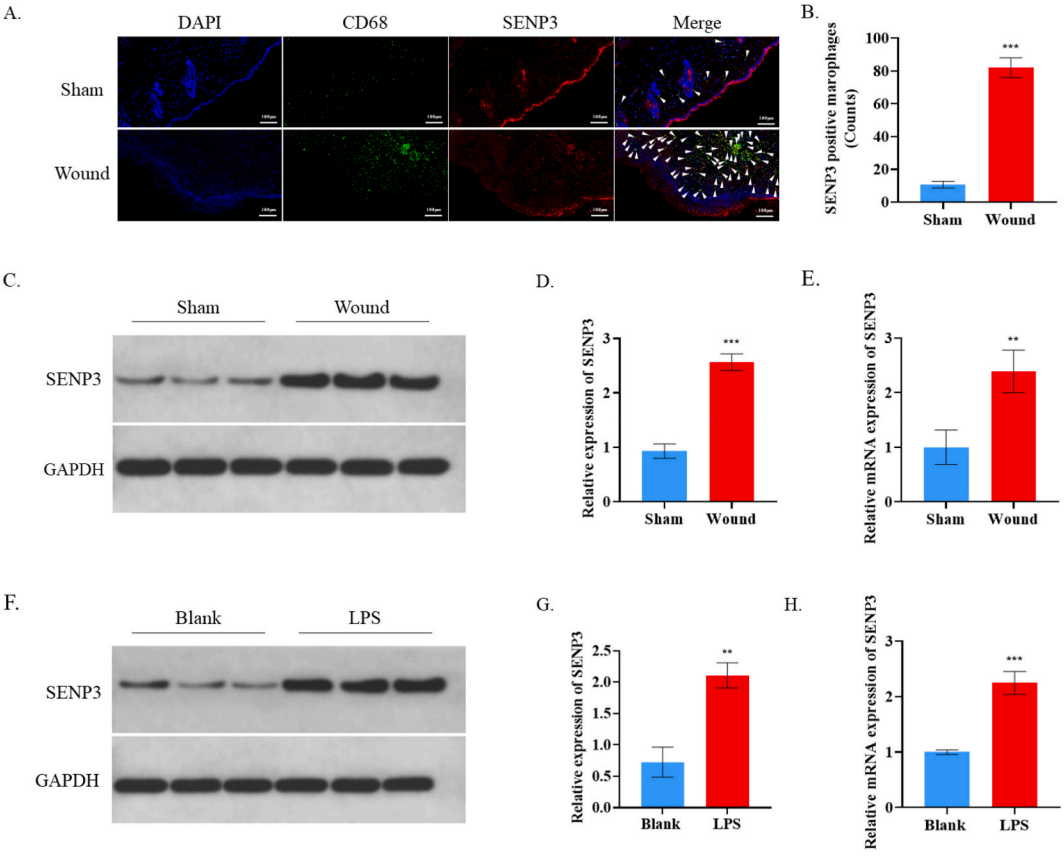

Fig. 1. SENP3 was significantly increased in macrophages during wound healing. (A–B) SENP3 expression was elevated in wound skin tissue according to immunofluorescence analysis. (*C*–E) SENP3 increased in wound skin tissue based on Western blot and RT−qPCR analysis. (F–H) SENP3 increased in wound skin tissue based on Western blot and RT−qPCR analysis. **, $P < 0.01$; ***, $P < 0.001$. SENP3, SUMO-specific protease 3; RT−qPCR, real-time polymerase chain reaction.

inflammatory cytokine transcription in primary BMDMs based on the levels of the cytokines in SENP3$^{fl/fl}$ and SENP3^{cKO} mice. The details are shown as follows, in the BMDMs of SENP3 cKO and SENP3$^{fl/fl}$ mice, SENP3 deficiency decreased the serum levels of the cytokines TNF-α and IL-1β ($P < 0.05$), while wounding also reduced the expression of IL-6, TNF-α and IL-1β ($P < 0.01$) (Fig. 2G). We used LPS to stimulate macrophages to simulate the inflammation of wound healing and found that the supernatant levels of cytokines were reduced in the BMDMs of SENP3 cKO mice compared with those of SENP3$^{fl/fl}$ mice ($P < 0.001$) (Fig. 2H). Therefore, SENP3 may play a role in inflammatory cytokine production in macrophages, indicating the correlation between SENP3 and inflammatory cytokines. In addition, we performed flowcytometry assay using F480 and CD206 marker to examine the M2 polarization rates of BMDMs from both SENP3$^{fl/fl}$ and SENP3^{cKO} mice. We found that the M2 polarization rate of SENP3$^{fl/fl}$ group was lower than that of SENP3^{cKO}

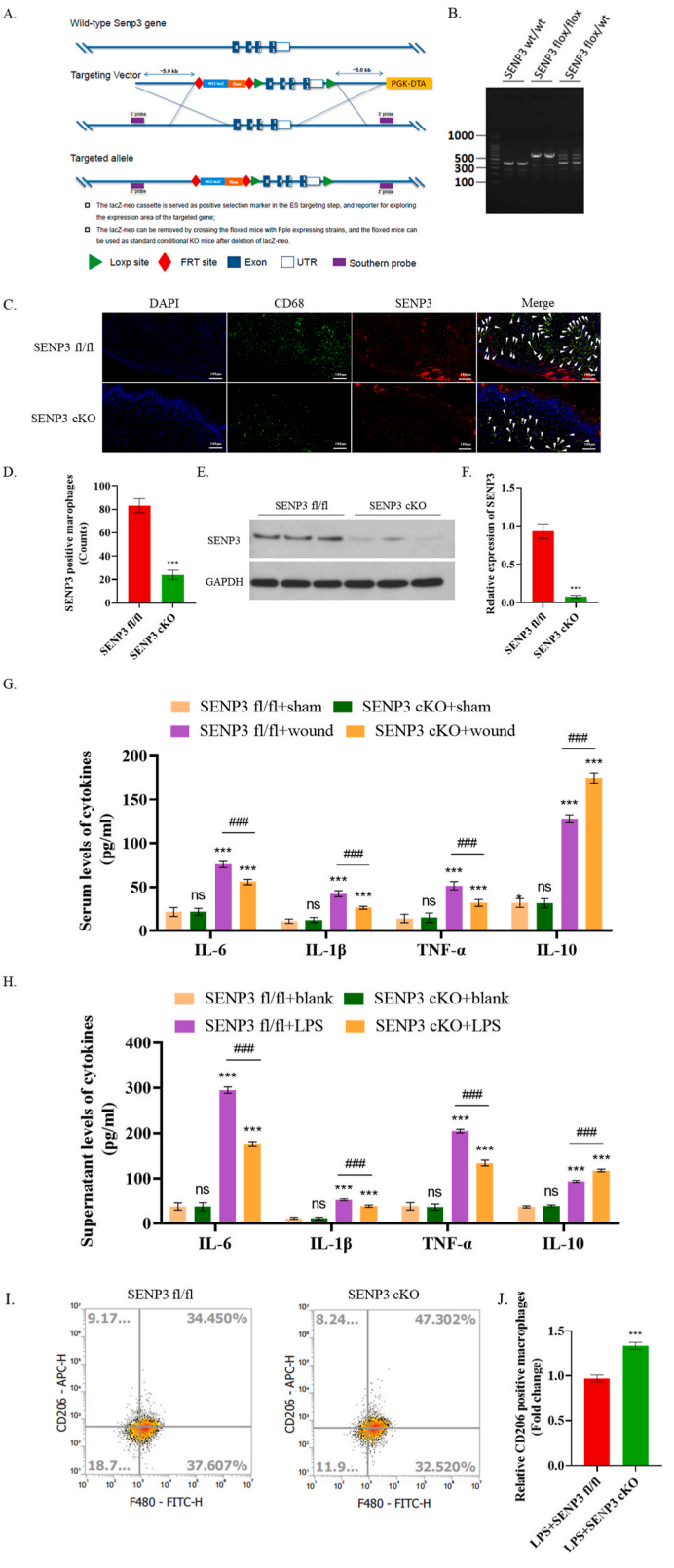

(caption on next page)

Fig. 2. SENP3 was conditionally knocked out in macrophages. (A) Schematic diagram of SENP3 conditional knockout mice. (B) Agarose gel electrophoresis results of genotype. (*C*–D) Immunofluorescence analysis indicated that SENP3 decreased in SENP3 cKO mice compared with SENP3$^{fl/fl}$ mice during wound healing. (*E*–F) Western blot analysis was used to validate SENP3 conditional knockout in macrophages. (G) ELISA analysis of serum (n = 10). (H) ELISA analysis of primary bone marrow macrophages (n = 10). (I) Flow cytometry assay of the M2 polarization of primary bone marrow macrophages. (J) Statistical analysis. *, P < 0.05; **, P < 0.01; ***, P < 0.001. SENP3, SUMO-specific protease 3; SENP3 cKO, SENP3 conditional knockout in macrophages; ELISA, enzyme-linked immunosorbent assay.

group (P < 0.001) (Fig. 2i-j). (K-L) F480. CD206 flow cytometry of SENP3 cKO mice.

2.3. Conditional SENP3 knockout in macrophages significantly promotes wound healing

After modeling full-thickness excisional skin wounds, we observed that SENP3 cKO mice showed a significantly smaller wound size than SENP3$^{fl/fl}$ mice during the wound healing process (Fig. 3A). The wound healing rate in SENP3 cKO mice on Days 1–12 was significantly higher than that in SENP3$^{fl/fl}$ mice (n = 6, P < 0.05) (Fig. 3B).

To further study how SENP3 deficiency promotes wound healing, we then observed the inflammatory response of wounds on Days 1, 3, and 7 by hematoxylin and eosin.

(HE) staining. On Day 1, a large number of inflammatory cells infiltrated around the wound of the SENP3$^{fl/fl}$ mice, whereas the infiltration of inflammatory cells in SENP3 cKO mice was significantly reduced. On Day 5, both groups showed a decreasing trend in the inflammatory response, and the infiltration of inflammatory cells in SENP3 cKO mice was significantly less than that in SENP3$^{fl/fl}$ mice. On Day 7, the number of inflammatory cells in both groups was significantly reduced compared to that on Days 1 and 5 (n = 6, P < 0.05) (Fig. 4A and B).

Masson staining in the wounds of SENP3 cKO mice showed a more collagen-rich wound bed, while sparse collagen deposition was noticeable in the wound beds of SENP3$^{fl/fl}$ mice wounds on Days 3–7 (n = 6, P < 0.05) (Fig. 4C and D).

CD31 immunohistochemistry (IHC) staining showed the angiogenesis of wounds on Days 3–7. The number of new blood vessels within the granulation tissue in SENP3$^{fl/fl}$ mice was significantly decreased compared with that in SENP3 cKO mice (n = 6, P < 0.05) (Fig. 4E and F).

Additionally, we labeled M1 and M2 macrophages with CD68 and CD206, respectively, by immunofluorescence staining to observe the dynamic changes in macrophages during wound healing. On Day 3, at the primary stage of wound healing, the number of M1 and M2 macrophages increased, and the inflammatory response was initiated. The number of M1 macrophages was greater than that of M2 macrophages. On Day 5, the inflammatory response exhibited a regression, and the number of M2 macrophages was greater than that of M1 macrophages, indicating the transformation from M1 to M2. Consistent with the results mentioned above, the polarization trend from M1 to M2 was strengthened in the SENP3 cKO group compared with the SENP3fl/fl group (n = 6, P < 0.05) (Fig. 4G–J). F480. CD206 flow cytometry of SENP3 cKO mice showed that the M2 polarization ratio of BMDMs from SENP3 cKO mice increased (n = 6, P

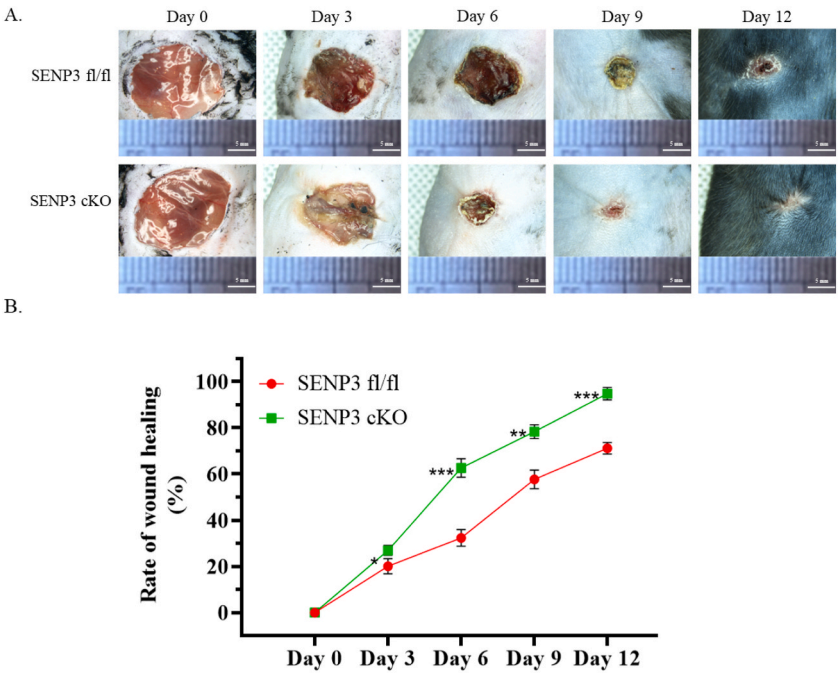

Fig. 3. Conditional SENP3 knockout significantly accelerated the wound healing process. (A) Representative images of the wound healing progress of the two groups on Days 0, 3, 6, 9 and 12. (B) Statistical analysis. *, P < 0.05. SENP3, SUMO-specific protease 3.

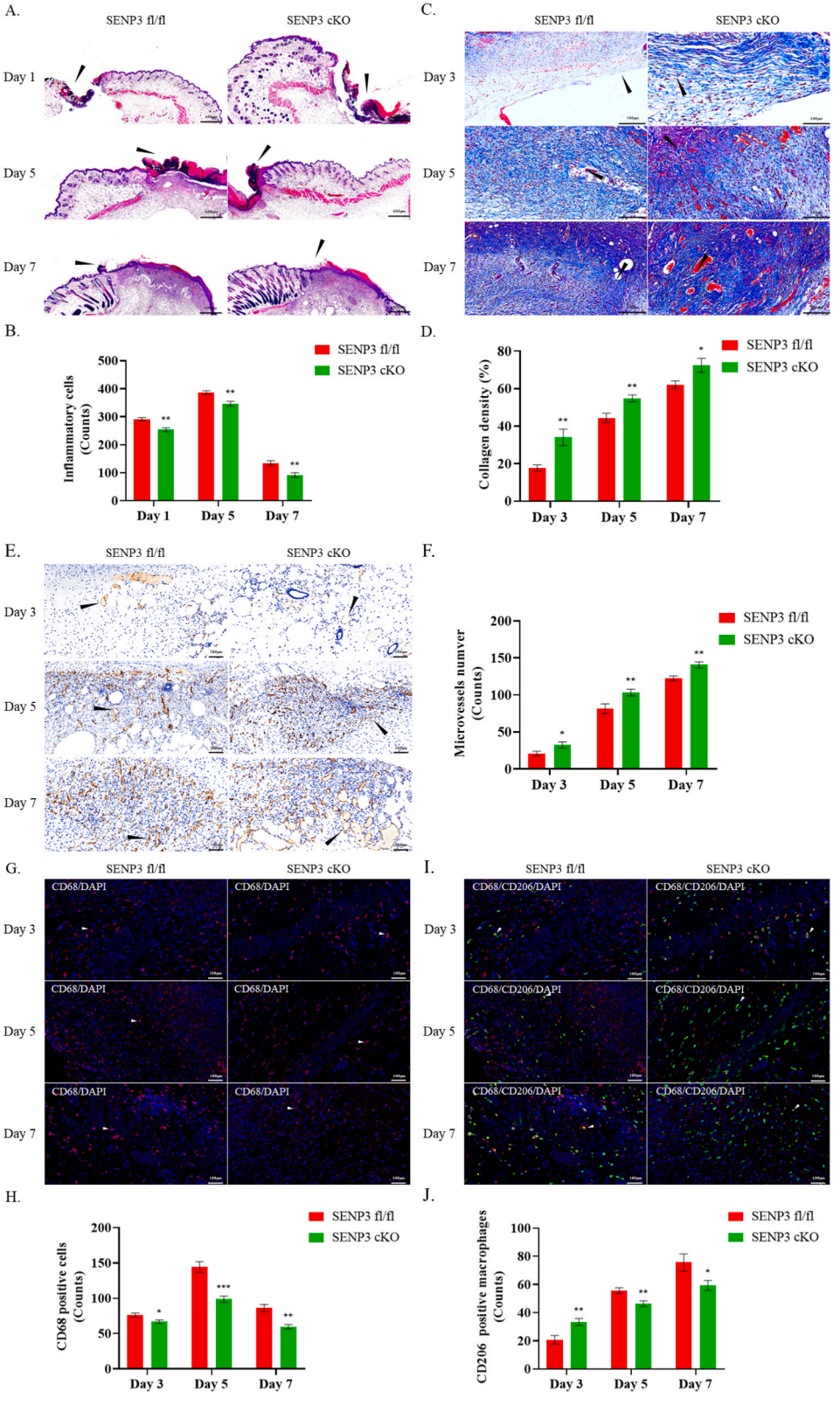

(caption on next page)

Fig. 4. Conditional SENP3 knockout promoted angiogenesis and M2 macrophage polarization. (A–B) HE staining showed the number of inflammatory cells. Scale bar = 600 μm. (*C*–D) Masson staining showed the collagen density. Scale bar = 100 μm. (*E*–F) Immunohistochemical staining of CD31 presented the microvessel number. Scale bar = 100 μm. (G–H) Immunofluorescent staining of CD68 showed the macrophage number. Scale bar = 100 μm. (I–J) Immunofluorescent staining of CD68 and CD206 colocalization showed the M2 macrophage number. Scale bar = 100 μm *, $P < 0.05$. SENP3, SUMO-specific protease 3; HE, hematoxylin and eosin.

< 0.05) (Fig. 4K-L).

2.4. SENP3 deficiency activates Smad6/IκB signaling in macrophages

GSEA of the RNA-sequencing dataset demonstrated a negative enrichment of wound healing and angiogenesis in macrophages with SENP3 knockout (Fig. 5A). RNA-sequencing data analysis revealed that the expression of Smad6 and IκBα (Nfkbia) was significantly increased in macrophages with SENP3 deficiency (Fig. 5B). Functional annotation analysis showed genes with ectopic expression between macrophages with or without SENP3 knockout. (Fig. 5C). Consistent results were obtained by Western blot and qRT−PCR ($P < 0.001$) (Fig. 5D and F). Additionally, the knockdown of SENP3 promoted the expression of TGFβ3 but did not affect the Smad7 expression in protein level (Fig. 5G–I). To the best of our knowledge, TGF-β was bidirectional in the inflammatory process, and TGF-β3 has been reported to promote wound healing and reduce scar tissue formation (Li et al., 2018). Meanwhile, Smad7 and Smad6, important regulators of TGFβ pathway expression, were up-regulated at the transcription level, but Western blot analysis confirmed that Smad7 was not changed at the protein level, while Smad6 was up-regulated at the protein level, indicating the potential relationship between Smad6 and inflammation.

2.5. Macrophage SENP3 conditional knockout elevated M2 polarization

Smad6 was reported to be a potential target in the pathological process of wound healing [15]. To evaluate the expression of Smad6 in different groups, we performed immunofluorescence analysis and Western blot analysis. The results of immunofluorescence analysis demonstrated that the expression of Smad6 was decreased in wound tissue and was elevated in the SENP3 cKO group ($n = 6$, $P < 0.001$) (Fig. 6A and B). Consistently, according to Western blot analysis, Smad6 was downregulated in BMDMs treated with LPSs and was upregulated by SENP3 conditional knockout. In addition, the protein level of IκB was suppressed by LPS treatment and enhanced in the SENP3 cKO group ($P < 0.001$) (Fig. 6C–E), indicating that SENP3 knockout can reverse the inhibitory effect on Smad6 exerted by LPS treatment.

2.6. SENP3 promotes inflammation via the smad6/IκB/p65 pathway

To determine whether SENP3 regulates inflammation through the Smad6/IκB/p65 signaling pathway, western blotting was performed to analyze the protein levels of molecules upstream and downstream of the Smad6/IκB/p65 signaling pathway in the BMDMs of SENP3 cKO and $SENP3^{fl/fl}$ mice. BMDMs were transfected with Smad6-specific and corresponding negative control siRNAs to construct si-Smad6 BMDMs. Subsequently, Western blot and RT−qPCR analyses were performed to determine Smad6 expression in these two groups (Fig. 7A and B). The elevated protein expression of IκB in SENP3 cKO macrophages was downregulated by si-Smad6, indicating the regulatory effect of Smad6 on IκB. The decreased protein expression of phosphorylated p65 (p-p65) in SENP3 cKO macrophages was upregulated by si-Smad6 ($P < 0.001$) (Fig. 7D–F). Furthermore, the supernatant levels of relative inflammatory cytokines, such as IL-6, IL-1β and TNF-α, were in accordance with the findings mentioned above ($P < 0.05$) (Fig. 7D). NF-κB was downregulated after SENP3 knockdown, and the level of IκB was increased, while IκB was downregulated and NF-κB was upregulated after si-smad6, which confirmed that SENP3 could regulate macrophage polarization by the Smad6/IκB/NF-Kb/P65 pathway ($P < 0.05$) (Fig. 7D). Under LPS stimulation, the expression of the anti-inflammatory factor IL-10 increased after SENP3 knockout, while the expression of IL-10 was downregulated after Smad6 knockout, reversing the effect of SENP3 knockout ($P < 0.05$) (Fig. 7G).

3. Discussion

Skin wound macrophages are key regulators of the innate immune response and critical facilitators of orchestrating the inflammatory response in wound healing [16]. In response to changes in the wound microenvironment, macrophages show considerable plasticity to acquire and exhibit diverse polarization states [17,18]. M2 macrophages, as a group of heterogeneous macrophages with anti-inflammatory effects, play an important role in pathophysiological processes such as the resolution of inflammation, the occurrence of hypersensitivity and the repair of damage [6,19]. The factors or cues in the wound microenvironment that drive such diversity to promote wound healing remain unclear at present. This study provides preliminary evidence demonstrating that the SUMO protease SENP3 regulates the inflammatory responses of macrophages in wound healing.

First, we verified that SENP3 is highly expressed during wound healing, indicating that SENP3 is positively correlated with wound healing. Furthermore, to simulate the inflammatory response in wound healing, we stimulated macrophages with LPS and found that the expression of SENP3 was also significantly increased during this process. In this study, we constructed macrophage SENP3 conditional knockout mice and a dorsal wound model and confirmed that during the wound healing process, the number of SENP3-positive M1 macrophages in SENP3 cKO mice decreased, indicating that SENP3 deletion in macrophages inhibits the production of

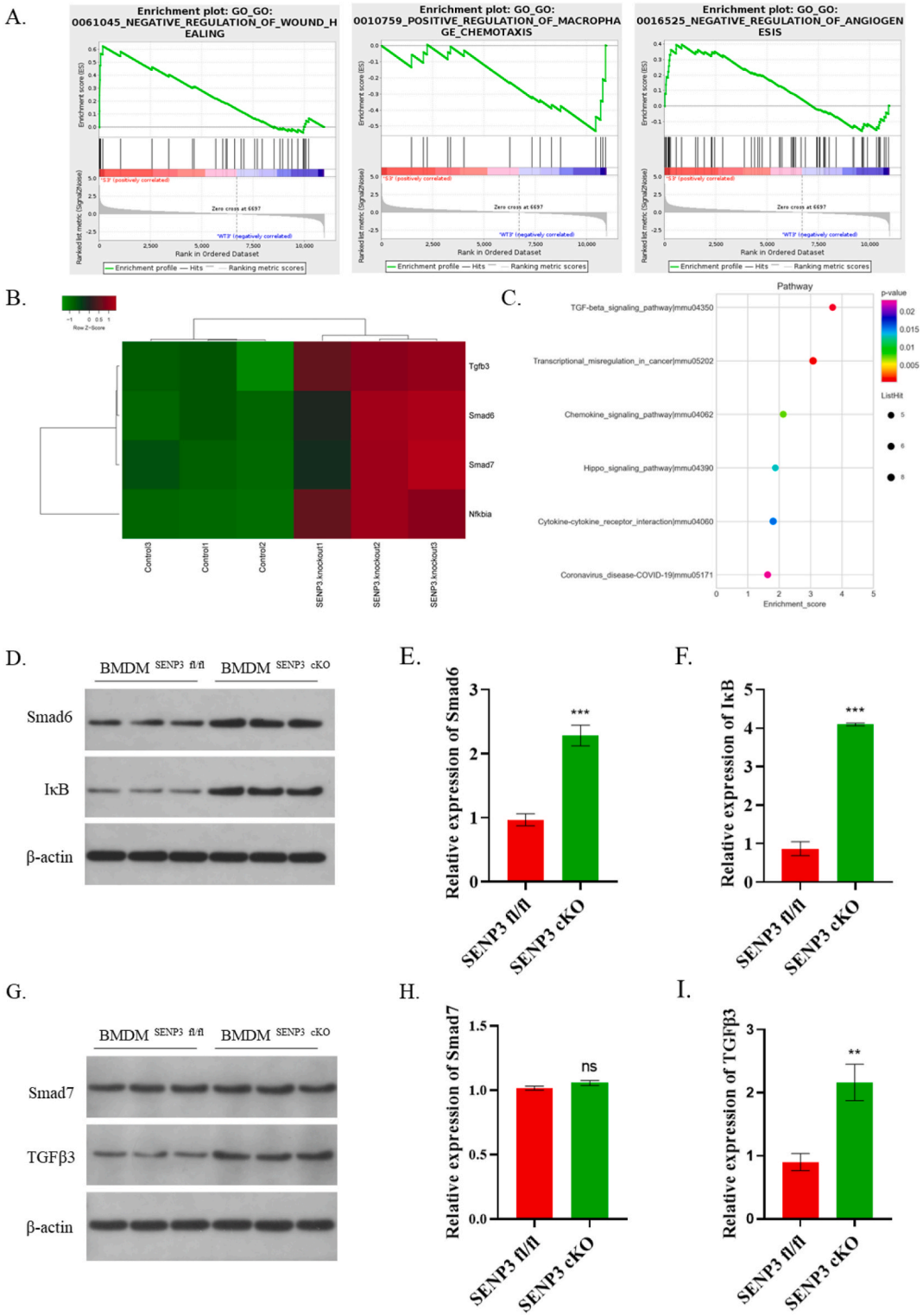

Fig. 5. SENP3 loss activated Smad6 signaling in macrophages. (A) An enrichment of wound healing and angiogenesis was negatively regulated in macrophages with SENP3$^{fl/fl}$. (B) RNA-sequencing data analysis revealed that Smad6 and IκBα (Nfkbia) expression was significantly increased in macrophages with SENP3 knockdown. (C) Functional annotation analysis of genes with ectopic expression between macrophages with or without SENP3 knockdown. (D–F) RT−qPCR and Western blot analysis were performed to evaluate Smad6 and IκBα expression in macrophages with or without SENP3 knockout. (G) Western blot analysis of Smad7 and TGFβ3. (H–I) Statistical analysis. Data were presented as mean ± s.d. *, $P < 0.05$; **, $P < 0.01$. SENP3, SUMO-specific protease 3; IκB, inhibitor of NF-κB; RT−qPCR, real-time polymerase chain reaction.

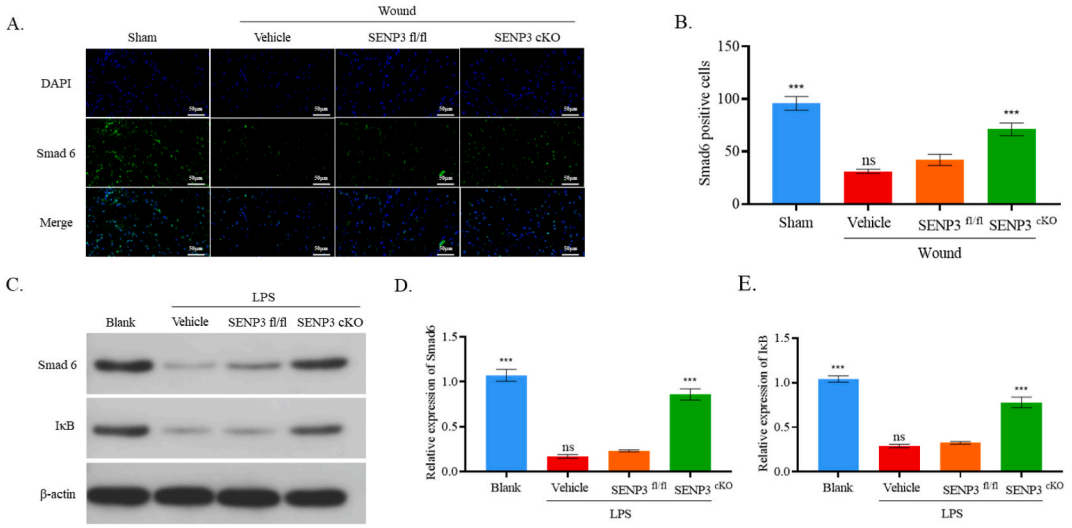

Fig. 6. Macrophage SENP3 conditional knockout elevated the M2 polarization Smad6/IκB expression suppressed by LPS treatment. (A–B) Immunofluorescence analysis indicated the expression of Smad6 in different groups. Scale bar = 50 μm. (*C*–E) Western blot and RT−qPCR analyses showed the expression of Smad6 in different groups. ***, P < 0.001. SENP3, SUMO-specific protease 3; IκB, inhibitor of NF-κB; LPS, lipopolysaccharide; RT−qPCR, real-time polymerase chain reaction.

M1 macrophages. The secretion of inflammatory cytokines was also reduced in serum and cellular supernatant, suggesting that SENP3 depletion suppressed the inflammatory response.

In recent years, it has been found that SUMOylation and SENP-mediated deSUMOylation have been linked to suppressed inflammation in macrophages, which efficiently regulates the functional activities and gene expression levels of related proteins and affects the development and outcome of inflammation [13,20–24]. Glass et al. contributed to the regulation of the transcriptional activity of inflammatory transcription factor complexes by SUMOylation of nuclear receptors in macrophages and found that upon activation of peroxisome proliferator-activated receptor gamma (PPARγ) and liver X receptors (LXRs) in macrophages, the modification of SUMO1 at Lys 77 and Lys 365 of PPAR-γ and the modification of SUMO2 at Lys 410 and Lys 448 of LXRs promote the transcriptional repression of the NCoR complex, thereby inhibiting downstream inflammatory factors [25,26]; additionally, SENP3 can remove the SUMOylation on LXRs, thereby releasing the transcriptional repression of the NCoR complex and promoting the expression of downstream inflammatory factors [27]. Kemper et al. reported that SUMO2 modification of macrophage farnesoid X receptor (FXR) can also promote the inhibitory function of transcriptional repression complexes, thereby inhibiting the expression of inflammatory factors [28]. Keiko Ozato et al. revealed that SUMO3 modification at Lys 310 of interferon regulatory factor 8 (IRF8) inhibits the expression of antiviral inflammatory factors in macrophages, while SENP1 can deactivate SUMOylation, thereby activating macrophages [29]. Lao et al. reported that SENP3 enhances the expression of inflammatory cytokines in response to LPS stimulation via MKK7 deSUMOylation [13]. Chen et al. showed that SENP3 mediates LPS-induced coagulation activation by upregulating monocyte/macrophage tissue factor production in a JNK-dependent manner [14]. These findings elucidate the roles of SUMOylation and SENPs in macrophage polarization and the inflammatory response, which will help understand the development of inflammation, thereby providing more effective treatment options.

To determine how M2 polarization by SENP3 loss affects wound healing, we observed the suppression of inflammation and promotion of angiogenesis and collagen remodeling. We also noticed that the inflammatory cytokines IL-6, TNF-α and IL-1β decreased both *in vivo* and *in vitro*. In the process of skin wound healing, M1 macrophages are mainly recruited from peripheral blood and infiltrate the wound site at 1–2 days soon after wound formation, and most M1 macrophages are polarized to M2 macrophages at 3 days postinjury [30,31]. Timely and adequate M2 macrophage polarization is crucial for the proinflammatory to anti-inflammatory transition in wound healing. A lack of M2 macrophages results in delayed wound healing [32]. Collagen remodeling is a key process in wound repair, in which M2 macrophages play a critical role [33,34]. Previous studies have also shown that M2 macrophages are strongly associated with angiogenesis [35,36], which is consistent with our results.

TGF-β protein expression was increased when the TGF-β pathway was activated. TGF-β is bidirectional in the inflammatory process, while TGF-β3 has been reported to promote wound healing and reduce scar tissue formation [37]. Additionally, Smad7 and Smad6, important regulators of TGFβ pathway expression, were upregulated at the transcriptional level, but Western blot confirmed that Smad7 was not changed while Smad6 was upregulated at the protein level [38,39]. Therefore, we used Smad6 as our downstream research object to clarify the important role of Smad6 in SENP3 regulation of macrophage polarization in wound healing.

To gain further insight into the underlying mechanism by which SENP3 loss inhibits inflammation in macrophages, we performed RNA sequencing and found that the expression levels of Smad6 and IκB were upregulated in SENP3-knockout macrophages. In addition, the protein levels of Smad6 and IκB increased in LPS-treated macrophages. Previous studies have shown that Smad6 upregulates IκB and inhibits p-p65 to repress inflammation [39,40], suggesting that SENP3 may play a role in the inhibition of

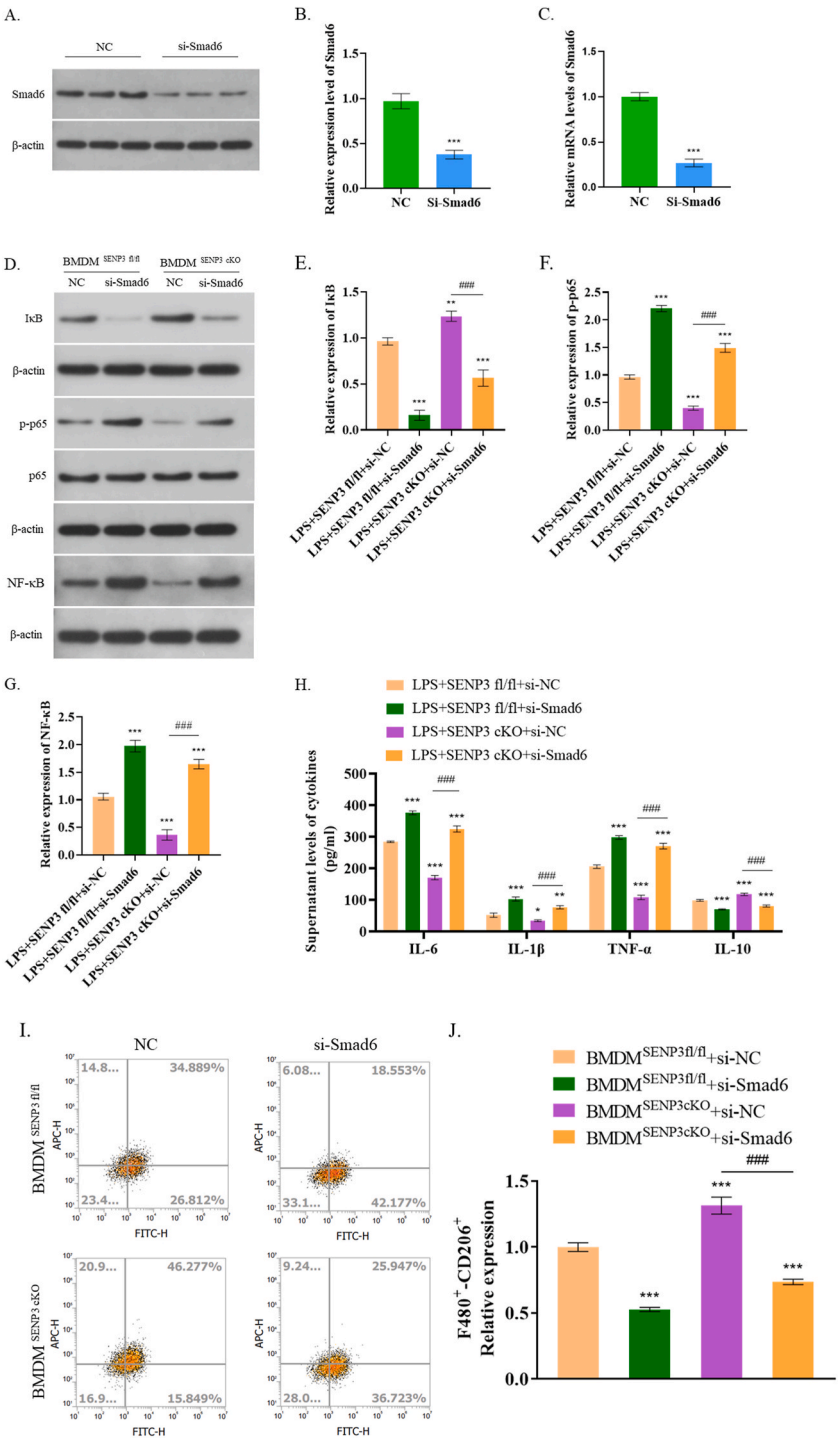

Fig. 7. SENP3 promotes inflammation via the Smad6/IκB/p65 pathway. (A–C) Western blot and RT−qPCR analyses indicated the expression level of Smad6 in control and si-Smad6 BMDMs. (D–F) Western blot analysis showed the protein levels of IκB and p-p65 in the four different groups. (G) ELISA analysis of inflammatory cytokines. (H–J) Flow cytometry analysis evaluated the ratio of M2 macrophages in the different groups. *, $P < 0.05$; ***, $P < 0.001$. SENP3, SUMO-specific protease 3; IκB, inhibitor of NF-κB; RT−qPCR, real-time polymerase chain reaction; BMDM, bone marrow-derived macrophages; p-p65, phosphorylation of p65; ELISA, enzyme-linked immunosorbent assay.

inflammation through the Smad6/IκB pathway. In addition, Smad6 has been demonstrated to suppress NF-κB activation and periodontal inflammation [39]. Previous work suggested that induction of Smad6 accelerated wound healing. Mechanistically, Smad6 is a novel target that activates bone morphogenetic protein 2 (BMP2) [15]. Therefore, to test the above hypothesis, we knocked out Smad6 in macrophages, which significantly inhibited the upregulation of IκB, while p-p65 was increased. Meanwhile, the decreased levels of inflammatory cytokines, such as IL-18, IL-6 and TNF-α, in the SENP3 cKO group were elevated by Smad6 knockdown, consistent with previous results. Previous studies have provided insights into NF-κb/IκB signaling, which exerts significant influences on the system-wide oxidative stress response, macrophage polarization and inflammation [41,42]. It was reported that the NF-κB/IκB signaling pathway played an important role in wound healing [43]. Suppression of the NF-κB/p65 pathway in fibroblasts promoted skin wound repair [44]. Hence, blockade of SENP3 repressed inflammation via the Smad6/IκB/p65 pathway, further implicating SENP3 as a promising therapeutic strategy in wound healing.

4. Conclusion

In summary, our study identified the key role of SENP3 in M2 macrophage polarization and wound healing as well as the underlying mechanism. Furthermore, we found that SENP3 deletion in macrophages promotes M2 polarization and accelerates wound healing through the Smad6/IκB/p65 signaling pathway, which may provide a therapeutic approach in wound healing.

5. Materials and methods

5.1. Mice

C57BL/6 mice (age, 6–8 weeks old) were purchased from Shanghai SLAC Laboratory Animal Co. Ltd. and were raised under specific pathogen-free conditions. C57BL/6 $Senp3^{+/-}$ mice were generated by BayGenomics (San Francisco, CA). C57BL/6 $Senp3^{flox}$ mice were generated by the Model Animal Research Center of Nanjing University (Nanjing, China). A neomycin cassette abutted with LacZ and an FRT sequence at the *N*-terminus of the exon 8-adjacent region was needed to produce an embryonic stem (ES) cell that aims at the vector with exons 8 and 11 adjoined by the loxP sequence. The positive ES cells, obtaining the vector through transfection/electroporation and verified by PCR/Southern blot analysis, were injected into C57BL/6 mice, which copulated with FLP-FRT mice afterward to eliminate LacZ and neomycin. Then, the 'purified' mice were crossed with Lyz2-cre C57BL/6 mice for further experiments. The mice were raised in a specific pathogen-free (SPF) animal laboratory at Shanghai Ninth People's Hospital and divided into two groups: SENP3 cKO mice formed the experimental group (n = 6), while SENP3 flox/flox (fl/fl) mice formed the control group (n = 6).

Animal experiments were in compliance with the national guidelines for the Care and Use of Laboratory Animals issued by the Ministry of Science and Technology of the People's Republic of China. All experimental procedures were approved by the Institutional Animal Care and Use Committee of Shanghai Ninth People's Hospital, Shanghai Jiao Tong University School of Medicine.

5.2. Wound-healing model

Mice were anesthetized by peritoneal injection with pentobarbital sodium (50 mg/kg; Boster, Wuhan, China). Two full-thickness wounds were made on the dorsum on each side of the midline using a sterile 12-mm biopsy punch (Miltex, New York, NY, USA). The wound healing of each group was digitally photographed from Day 0 to Day 12. The rate of wound healing [(Day 0 wound area - wound area)/Day 0 wound area × 100%] was used to evaluate the wound healing process. Wound area was analyzed with ImageJ software [National Institutes of Health (NIH), Bethesda, MD, USA]. The wound tissue for hematoxylin-eosin (HE) and immunohistochemistry (IHC) staining was extracted at Day 1, Day 3, Day 5 and Day 7 after modeling.

5.3. Cell isolation and transfection

Primary murine macrophages were differentiated from bone marrow harvested from SENP3 $^{(fl/fl)}$ and SENP3 cKO mice. The harvested marrow was femoral and tibial bones treated with ACK lysis buffer (Thermo Fisher Scientific, Waltham, MA, USA) and plated in tissue culture flasks. Naive macrophages were generated by cell culture in Dulbecco's modified Eagle's medium (DMEM) (Thermo Fisher Scientific, Waltham, MA, USA) containing 10% fetal bovine serum (Thermo Fisher Scientific, Waltham, MA, USA), 50 U/mL penicillin-50 μg/mL streptomycin (Thermo Fisher Scientific, Waltham, MA, USA), and 30 ng/mL murine recombinant macrophage colony stimulating factor (*M*-CSF, PeproTech, Rocky Hill, NJ) for 7 days. Cells were then isolated with Accutase and plated onto modified Ti surfaces or tissue culture polystyrene (TCPS) in 24-well plates for subsequent experiments. For the knockdown experiment, cells were transfected with siRNA oligonucleotides using the Lipofectamine RNAiMAX Transfection Reagent (Invitrogen, Waltham, MA). (Smad6)-specific and corresponding negative control (NC) siRNAs were obtained from Guangzhou RiboBio.

5.4. Quantitative real-time PCR

Total RNA was extracted from tissues or cultured cells using TRIzol (Invitrogen, Carlsbad, CA, USA). Complementary DNA (cDNA) was obtained by reverse transcribing total RNA with the PrimeScript RT Reagent Kit (Takara Bio Inc., Shiga, Japan). Quantitative real-time PCR was performed in an ABI 7500 Real-Time PCR system (Applied Biosystems, Foster City, CA, USA) using SYBR Green Real-time PCR Master Mix (Yeasen, Shanghai, China). The primer sequences are shown in Supplementary Table 1.

5.5. Western blotting analysis

Skin tissue and cellular protein extraction and Western blotting were performed according to our previous protocols [45]. All the antibodies are presented in Supplementary Table 2.

5.6. Immunohistochemistry and immunofluorescence staining

Immunohistochemistry performed on paraffin sections and immunofluorescence staining performed on cells were described in our previous study [45]. For tissue immunofluorescence staining, sections were permeabilized using 0.2% Triton X-100 before blocking using 20% goat serum and then incubated with primary antibodies at 4 °C overnight. The sections were then incubated with Alexa Fluor 594/488-conjugated anti-rabbit secondary antibodies (Jackson ImmunoResearch, West Grove, PA, USA). DAPI was used for nuclear staining. The numbers of immunofluorescence-positive cells were quantified from five microscopic fields (Zeiss).

5.7. ELISA

IL-6, TNF-α and IL-1β concentrations in the serum and cellular supernatant were examined using murine ELISA kits (eBioscience Systems) according to the manufacturer's protocol. Supernatants were stored at 80 °C before measurement.

5.8. Flow cytometry

Cells were incubated with primary antibodies for 30 min on ice in the dark, followed by washing and analysis on an LSRII flow cytometer (BD Biosciences). Data analysis was performed by FACSDiva (version 6.1.1; BD Biosciences) and Prism 5.0 (GraphPad).

5.9. RNA sequencing and bioinformatics analysis

Total RNA was extracted from bone marrow-derived macrophages (BMDMs) from $SENP3^{fl/fl}$ and SENP3 cKO mice (three randomly selected samples from each group) using TRIzol (Invitrogen, USA) according to the manufacturer's instructions. After quality evaluation, total RNA samples were enriched by Oligo dT (rRNA removal), and then the KAPA Stranded RNA-Seq library Prep Kit (Illumina) was selected to construct the RNA-seq library. Then, the quality of the constructed libraries was evaluated by an Agilent 2100 BioAnalyzer and quantified using the RT−qPCR method. FastQC software was applied to decapitate reads, and then Hisat2 software was used to compare the reference genome. The FPKM calculation of gene level and transcript level was performed using R software Ballgown, and the differentially expressed genes (DEGs) of two groups were screened out based on fold change (FC) and p values ($FC \geq 1.5$ and p value < 0.05). In addition, GO analysis was performed to investigate three functional domains: molecular function (MF), cellular component (CC) and biological process (BP). KEGG pathway analysis was performed to functionally determine and map genes.

5.10. Lipopolysaccharide stimulation

Inflammation is a significant component of wound healing. Lipopolysaccharide (LPS) stimulation was applied to initiate the pathological process in BMDMs according to a previous study [46]. Concretely, BMDMs from $SENP3^{fl/fl}$ and SENP3 cKO mice were primed with 100 ng/mL LPS (Sigma, L8274) for 12 h. Afterward, the supernatant and BMDMs were collected, and the expression of corresponding genes was investigated by RT−qPCR, Western blot and ELISA.

5.11. Statistical analysis

All *in vitro* experiments were repeated at least three times. All statistical analyses were performed in GraphPad Prism 7 (San Diego, CA, USA). Student's *t*-test, one-way analysis of variance (ANOVA) and two-way ANOVA were used for comparisons. A value of $P < 0.05$ was considered statistically significant.

Author contribution statement

Yiwen Ma, Jiateng Hu, Xingjuan Xue, Jianmin Gu and Yuyan Pan: Conceived and designed the experiments.
Xingjuan Xue, Jianmin Gu, Yuyan Pan and Jun Yang: Analyzed and interpreted the data, Wrote the paper.
Yiwen Ma and Jiateng Hu: Contributed reagents, materials, analysis tools or data, Wrote the paper.
Yiwen Ma, Jiateng Hu and Yuyan Pan: Performed the experiments, Wrote the paper.
Lin Yuan; Bin Su; Tong Zhang: Contributed reagents, materials, analysis tools or data; Wrote the paper.

Funding statement

Proffessor Yuyan Pan was supported by National Natural Science Foundation of China [82102333].

Data availability statement

Data will be made available on request.

Additional information

Supplementary content related to this article has been published online at [URL].

Declaration of competing interest

The authors declare that they have no known competing financial interests or personal relationships that could have appeared to influence the work reported in this paper.

Appendix A. Supplementary data

Supplementary data to this article can be found online at https://doi.org/10.1016/j.heliyon.2023.e15584.

References

[1] J. Guest, K. Vowden, P. Vowden, The health economic burden that acute and chronic wounds impose on an average clinical commissioning group/health board in the UK, J. Wound Care 26 (2017) 292–303, https://doi.org/10.12968/jowc.2017.26.6.292.

[2] N. Kosaric, H. Kiwanuka, G. Gurtner, Stem cell therapies for wound healing, Expet Opin. Biol. Ther. 19 (2019) 575–585, https://doi.org/10.1080/14712598.2019.1596257.

[3] G. Han, R. Ceilley, Chronic wound healing: a review of current management and treatments, Adv. Ther. 34 (2017) 599–610, https://doi.org/10.1007/s12325-017-0478-y.

[4] C. Minutti, J. Knipper, J. Allen, D. Zaiss, Tissue-specific contribution of macrophages to wound healing, Semin. Cell Dev. Biol. 61 (2017) 3–11, https://doi.org/10.1016/j.semcdb.2016.08.006.

[5] F. Martinez, A. Sica, A. Mantovani, M. Locati, Macrophage activation and polarization, Front. Biosci. : J. Vis. Literacy 13 (2008) 453–461, https://doi.org/10.2741/2692.

[6] A. Louiselle, S. Niemiec, C. Zgheib, K. Liechty, Macrophage polarization and diabetic wound healing, Transl. Res. : J. Lab. Clin. Med. 236 (2021) 109–116, https://doi.org/10.1016/j.trsl.2021.05.006.

[7] S. Gordon, Alternative activation of macrophages, Nat. Rev. Immunol. 3 (2003) 23–35, https://doi.org/10.1038/nri978.

[8] S. Basu Mallik, B. Jayashree, R. Shenoy, Epigenetic modulation of macrophage polarization- perspectives in diabetic wounds, J. Diabetes Complicat. 32 (2018) 524–530, https://doi.org/10.1016/j.jdiacomp.2018.01.015.

[9] J. Liu, Q. Wang, Y. Kang, S. Xu, D. Pang, Unconventional protein post-translational modifications: the helmsmen in breast cancer, Cell Biosci. 12 (2022) 22, https://doi.org/10.1186/s13578-022-00756-z.

[10] E. Yeh, SUMOylation and De-SUMOylation: wrestling with life's processes, J. Biol. Chem. 284 (2009) 8223–8227, https://doi.org/10.1074/jbc.R800050200.

[11] S. Yan, X. Sun, B. Xiang, H. Cang, X. Kang, Y. Chen, H. Li, G. Shi, E. Yeh, B. Wang, et al., Redox regulation of the stability of the SUMO protease SENP3 via interactions with CHIP and Hsp 90, EMBO J. 29 (2010) 3773–3786, https://doi.org/10.1038/emboj.2010.245.

[12] C. Huang, Y. Han, Y. Wang, X. Sun, S. Yan, E. Yeh, Y. Chen, H. Cang, H. Li, G. Shi, et al., SENP3 is responsible for HIF-1 transactivation under mild oxidative stress via p300 de-SUMOylation, EMBO J. 28 (2009) 2748–2762, https://doi.org/10.1038/emboj.2009.210.

[13] Y. Lao, K. Yang, Z. Wang, X. Sun, Q. Zou, X. Yu, J. Cheng, X. Tong, E. Yeh, J. Yang, J. Yi, DeSUMOylation of MKK7 kinase by the SUMO2/3 protease SENP3 potentiates lipopolysaccharide-induced inflammatory signaling in macrophages, J. Biol. Chem. 293 (2018) 3965–3980, https://doi.org/10.1074/jbc.M117.816769.

[14] X. Chen, Y. Lao, J. Yi, J. Yang, S. He, Y. Chen, SENP3 in monocytes/macrophages up-regulates tissue factor and mediates lipopolysaccharide-induced acute lung injury by enhancing JNK phosphorylation, J. Cell Mol. Med. 24 (2020) 5454–5462, https://doi.org/10.1111/jcmm.15199.

[15] B. Mi, L. Chen, Y. Xiong, C. Yan, H. Xue, A. Panayi, J. Liu, L. Hu, Y. Hu, F. Cao, et al., Saliva exosomes-derived UBE2O mRNA promotes angiogenesis in cutaneous wounds by targeting SMAD6, J. Nanobiotechnol. 18 (2020) 68, https://doi.org/10.1186/s12951-020-00624-3.

[16] A. Das, M. Sinha, S. Datta, M. Abas, S. Chaffee, C. Sen, S. Roy, Monocyte and macrophage plasticity in tissue repair and regeneration, Am. J. Pathol. 185 (2015) 2596–2606, https://doi.org/10.1016/j.ajpath.2015.06.001.

[17] S. Brancato, J. Albina, Wound macrophages as key regulators of repair: origin, phenotype, and function, Am. J. Pathol. 178 (2011) 19–25, https://doi.org/10.1016/j.ajpath.2010.08.003.

[18] M. Crane, J. Daley, O. van Houtte, S. Brancato, W. Henry, J. Albina, The monocyte to macrophage transition in the murine sterile wound, PLoS One 9 (2014), e86660, https://doi.org/10.1371/journal.pone.0086660.

[19] C. Ferrante, S. Leibovich, Regulation of macrophage polarization and wound healing, Adv. Wound Care 1 (2012) 10–16, https://doi.org/10.1089/wound.2011.0307.

[20] G. Pascual, A. Fong, S. Ogawa, A. Gamliel, A. Li, V. Perissi, D. Rose, T. Willson, M. Rosenfeld, C. Glass, A SUMOylation-dependent pathway mediates transrepression of inflammatory response genes by PPAR-gamma, Nature 437 (2005) 759–763, https://doi.org/10.1038/nature03988.

[21] T.-H. Chang, Kanno Tailor, Ozato, The small ubiquitin-like modifier-deconjugating enzyme sentrin-specific peptidase 1 switches IFN regulatory factor 8 from a repressor to an activator during macrophage activation, J. Immunol.: Official J. Am. Assoc. Immunol. 189 (2012) 3548–3556.

[22] X. Chen, Y. Lao, J. Yi, J. Yang, Y. Chen, SENP3 in monocytes/macrophages up-regulates tissue factor and mediates lipopolysaccharide-induced acute lung injury by enhancing JNK phosphorylation, J. Cell Mol. Med. 24 (2020).

[23] T.J. Gross, L.S. Powers, R.L. Boudreau, B. Brink, A. Reisetter, K. Goel, A.K. Gerke, I.H. Hassan, M.M. Monick, A MicroRNA processing defect in smokers' macrophages is linked to SUMOylation of the endonuclease DICER, J. Biol. Chem.108 (2014) 12823–12834.

[24] S.S. Im, T.F. Osborne, Liver X receptors in atherosclerosis and inflammation, Circ. Res. 108 (2011) 996–1001.

[25] G. Pascual, A.L. Fong, S. Ogawa, A. Gamliel, A.C. Li, V. Perissi, D.W. Rose, T.M. Willson, M.G. Rosenfeld, C.K. Glass, A SUMOylation-dependent pathway mediates transrepression of inflammatory response genes by PPAR-gamma, Nature 437 (2005) 759–763, https://doi.org/10.1038/nature03988.

[26] S. Ghisletti, W. Huang, S. Ogawa, G. Pascual, M.E. Lin, T.M. Willson, M.G. Rosenfeld, C.K. Glass, Parallel SUMOylation-dependent pathways mediate gene- and signal-specific transrepression by LXRs and PPARgamma, Mol. Cell 25 (2007) 57–70, https://doi.org/10.1016/j.molcel.2006.11.022.

[27] W. Huang, S. Ghisletti, K. Saijo, M. Gandhi, M. Aouadi, G.J. Tesz, D.X. Zhang, J. Yao, M.P. Czech, B.L. Goode, et al., Coronin 2A mediates actin-dependent de-repression of inflammatory response genes, Nature 470 (2011) 414–418, https://doi.org/10.1038/nature09703.

[28] D.H. Kim, Z. Xiao, S. Kwon, X. Sun, D. Ryerson, D. Tkac, P. Ma, S.Y. Wu, C.M. Chiang, E. Zhou, et al., A dysregulated acetyl/SUMO switch of FXR promotes hepatic inflammation in obesity, EMBO J. 34 (2015) 184–199, https://doi.org/10.15252/embj.201489527.
[29] T.H. Chang, S. Xu, P. Tailor, T. Kanno, K. Ozato, The small ubiquitin-like modifier-deconjugating enzyme sentrin-specific peptidase 1 switches IFN regulatory factor 8 from a repressor to an activator during macrophage activation, J. Immunol. 189 (2012) 3548–3556, https://doi.org/10.4049/jimmunol.1201104.
[30] F. Tacke, G. Randolph, Migratory fate and differentiation of blood monocyte subsets, Immunobiology 211 (2006) 609–618, https://doi.org/10.1016/j.imbio.2006.05.025.
[31] F. Ginhoux, F. Tacke, V. Angeli, M. Bogunovic, M. Loubeau, X. Dai, E. Stanley, G. Randolph, M. Merad, Langerhans cells arise from monocytes in vivo, Nat. Immunol. 7 (2006) 265–273, https://doi.org/10.1038/ni1307.
[32] T. Wynn, K. Vannella, Macrophages in tissue repair, regeneration, and fibrosis, Immunity 44 (2016) 450–462, https://doi.org/10.1016/j.immuni.2016.02.015.
[33] K. Motz, I. Lina, M. Murphy, V. Drake, R. Davis, H. Tsai, M. Feeley, L. Yin, D. Ding, A. Hillel, M2 macrophages promote collagen expression and synthesis in laryngotracheal stenosis fibroblasts, Laryngoscope 131 (2021) E346–E353, https://doi.org/10.1002/lary.28980.
[34] S. Gu, H. Dai, X. Zhao, C. Gui, J. Gui, AKT3 deficiency in M2 macrophages impairs cutaneous wound healing by disrupting tissue remodeling, Aging 12 (2020) 6928–6946, https://doi.org/10.18632/aging.103051.
[35] I. Larionova, E. Kazakova, T. Gerashchenko, J. Kzhyshkowska, New angiogenic regulators produced by TAMs: perspective for targeting tumor angiogenesis, Cancers 13 (2021), https://doi.org/10.3390/cancers13133253.
[36] T. Ueta, K. Ishihara, S. Notomi, J. Lee, D. Maidana, N. Efstathiou, Y. Murakami, E. Hasegawa, K. Azuma, T. Toyono, et al., RIP1 kinase mediates angiogenesis by modulating macrophages in experimental neovascularization, Proc. Natl. Acad. Sci. U. S. A 116 (2019) 23705–23713, https://doi.org/10.1073/pnas.1908355116.
[37] M. Li, L. Qiu, W. Hu, X. Deng, H. Xu, Y. Cao, Z. Xiao, L. Peng, S. Johnson, L. Alexey, et al., Genetically-modified bone mesenchymal stem cells with TGF-β improve wound healing and reduce scar tissue formation in a rabbit model, Exp. Cell Res. 367 (2018) 24–29, https://doi.org/10.1016/j.yexcr.2018.02.006.
[38] F. Zhang, C. Sodroski, H. Cha, Q. Li, T. Liang, Infection of hepatocytes with HCV increases cell surface levels of heparan sulfate proteoglycans, uptake of cholesterol and lipoprotein, and virus entry by up-regulating SMAD6 and SMAD7, Gastroenterology 152 (2017) 257–270.e257, https://doi.org/10.1053/j.gastro.2016.09.033.
[39] T. Zhang, J. Wu, N. Ungvijanpunya, O. Jackson-Weaver, Y. Gou, J. Feng, T. Ho, Y. Shen, J. Liu, S. Richard, et al., Smad6 methylation represses NFκB activation and periodontal inflammation, J. Dent. Res. 97 (2018) 810–819, https://doi.org/10.1177/0022034518755688.
[40] Y. Wang, M. Li, L. Chen, H. Bian, X. Chen, H. Zheng, P. Yang, Q. Chen, H. Xu, Natural killer cell-derived exosomal miR-1249-3p attenuates insulin resistance and inflammation in mouse models of type 2 diabetes, Signal Transduct. Targeted Ther. 6 (2021) 409, https://doi.org/10.1038/s41392-021-00805-y.
[41] H. Sies, C. Berndt, D.P. Jones, Oxidative stress, Annu. Rev. Biochem. 86 (2017) 715–748, https://doi.org/10.1146/annurev-biochem-061516-045037.
[42] J. Yang, G. Chen, T.W. Guo, W.Y. Qin, P. Jia, Simiao Wan attenuates monosodium urate crystal-induced arthritis in rats through contributing to macrophage M2 polarization, J. Ethnopharmacol. 275 (2021), 114123, https://doi.org/10.1016/j.jep.2021.114123.
[43] X. Jiang, Z. Yao, K. Wang, L. Lou, K. Xue, J. Chen, G. Zhang, Y. Zhang, J. Du, C. Lin, J. Xiao, MDL-800, the SIRT6 activator, suppresses inflammation via the NF-B pathway and promotes angiogenesis to accelerate cutaneous wound healing in mice, Oxid. Med. Cell. Longev. 2022 (2022) 1–14, https://doi.org/10.1155/2022/1619651.
[44] Y. Shen, Z. Zhu, W. Cong, M. Jiang, J. Wang, X. Chen, N. Wang, Y. Yu, Y. Dong, Z. Liu, et al., Phosphorylation of α-catenin(S641) suppresses the NF-κB pathway in fibroblasts to activate skin wound repair, J. Invest. Dermatol. 142 (2022) 1714–1724, https://doi.org/10.1016/j.jid.2021.09.037.
[45] Y. Pan, Q. Wang, W. Luan, Y. Shi, J. Liu, F. Qi, Kindlin-2 regulates the differentiation of 3T3-L1 preadipocytes: implications for wound healing, Ann. Transl. Med. 9 (2021) 348, https://doi.org/10.21037/atm-21-176.
[46] B. Zhang, H. Chen, J. Ouyang, Y. Xie, L. Chen, Q. Tan, X. Du, N. Su, Z. Ni, L. Chen, SQSTM1-dependent autophagic degradation of PKM2 inhibits the production of mature IL1B/IL-1β and contributes to LIPUS-mediated anti-inflammatory effect, Autophagy 16 (2020) 1262–1278, https://doi.org/10.1080/15548627.2019.1664705.